

Angular and velocity distributions of the HD^+ and D_2^+ fragments from HD_2^+ colliding with He at energies of 1 to 5 keV

I. Alvarez, H. Martínez, C. Cisneros, and J. de Urquijo

Instituto de Física, Universidad Nacional Autónoma de México, P.O. Box 139-B, 62191

Cuernavaca Morelos, Mexico

(Received 11 September 1990)

The angular and velocity distributions of the HD^+ and D_2^+ fragments resulting from collision-induced dissociation of the HD_2^+ molecular ion incident on He have been measured in the energy range 1–5 keV. These distributions were used to determine the binding energy of HD_2^+ , some of the main transitions involved in the dissociation process, and the total cross sections for the production of both fragments.

PACS number(s): 35.20.Vf, 35.20.Gs, 34.50.Lf

I. INTRODUCTION

The H_3^+ molecular ion and its isotopic variants HD_2^+ , H_2D^+ , and D_3^+ are the simplest polyatomic ions known regarding electronic structure. As examples of the great relevance for their study one can mention (i) the chemistry of dense molecular clouds in interstellar space [1,2], (ii) the heating or cooling of the clouds, (iii) in astrophysics, a knowledge of their vibrational and rotational spectra is very important [3,4], and (iv) in ionized plasmas, a knowledge of their dissociative recombination is fundamental [5].

HD_2^+ has been the least-studied ion of the hydrogenic family. To our knowledge, work has been focused in the following areas: in collision physics [6,7], the cross sections for the production of positive and negative ions, in the energy range of 40 to 600 keV, have been measured in several target gases as well as the Balmer lines H_β and D_β produced using the beam-foil technique [8]. Total cross sections for the dissociative-recombination process were measured by Mitchell *et al.* [5] who found them to be different for H_3^+ and D_3^+ . In the field of spectroscopy, Carrington and Kennedy [9] noticed that for identical frequency ranges the infrared predissociation spectra of HD_2^+ determined by monitoring either H^+ or D^+ fragment ions were different. By studying the chemical process $\text{H} + \text{D}_2$, Colling *et al.* [10] observed the transition-state HD_2^{2+} . The vibrational spectra and the Einstein coefficients for relevant transitions were calculated by Carney and Porter by *ab initio* calculations [11]. The photodissociation of the HD_2^+ molecule was performed by Berlinger *et al.* [12] with the result that there is a tendency to favor the production of the H^+ fragment when the molecule has a total angular momentum $J \leq 27$, whereas D^+ is formed mainly when $J \geq 30$. From these results, the differences in the H^+ and D^+ spectra observed by Carrington could be explained.

The purpose of this paper is to present our experimental data on the production of the D_2^+ and HD^+ diatomic

ionic fragments by collision-induced dissociation of HD_2^+ in He, in the energy range from 1 to 5 keV. Over this energy range we report the angular distributions, the absolute total cross sections, and the energy distributions at a projectile energy of 3 keV, followed by a discussion of the results.

II. EXPERIMENTAL APPARATUS

The experimental apparatus has been described elsewhere [13]. The HD_2^+ molecular ions were formed in a Colutron-type ion source. Mixing equal quantities of H_2 and D_2 in the ion source gas feed provided an adequate beam of HD_2^+ , which was electrostatically accelerated to energies of 1 to 5 keV. The selected molecular ion beam was velocity analyzed by a Wien filter, passed through a series of collimators before it entered the gas target cell, which was a cylinder 2.5 cm in length and 2.5 cm in diameter with a 1 mm entrance aperture and a 2-mm-wide, 6-mm-long exit aperture. All apertures and slits had knife edges. Path lengths and apertures gave the system an overall angular resolution of 0.1° .

The target cell was mounted in a computer-controlled vacuum chamber such that the detector assembly could be rotated about the center of the gas cell. Located 47 cm away from the gas cell was the detector assembly: a Harrower-type parallel-plate analyzer [14] with 0.36-mm entrance aperture and a channel-electron multiplier (CEM) attached to its exit end. The beam entered the uniform field at an angle of 45° . By replacing the collimator located in the front of the CEM, this analyzer was used to measure both angular and energy distributions of the products. To measure the angular distributions, the collimator in front of the CEM was an orifice of 1-cm in diameter, while a slit 1-cm-long and 0.01-mm-wide was placed in front of the CEM for energy-distribution measurements.

The energy distributions were obtained by varying the voltage on the analyzer; its calculated energy resolution was $\Delta\varepsilon/\varepsilon = 4.5 \times 10^{-3}$.

III. MEASUREMENT TECHNIQUES

The measured quantities were I_0 , the number of HD_2^+ ions incident per unit area per second; n , the number of helium atoms per unit volume; l , the effective length of the scattering chamber; and $I_f(\theta, \phi)$, the number of fragments of type f (i.e., D_2^+ or HD^+) per unit solid angle per second detected at angles (θ, ϕ) with respect to the incident beam direction. With these measurements, the quantity

$$\frac{d\sigma_f}{d\omega} = \frac{I_f(\theta, \phi)}{I_0 n l} \quad (1)$$

was evaluated. Although $d\sigma_f/d\omega$ formally looks like a differential cross section and is measured as such, it is not a "differential scattering" cross section. The fragment detected at angle θ has not been "scattered." The substantial angle at which a fragment reaches the detector is due to the transverse component of the velocity acquired in the dissociation process. This follows from one of the hypotheses of the two-step model of dissociation, namely that the deflection of the center of mass of the molecular ion is negligible [15]. Figures 1 and 2 exhibit the "differential cross sections" of the molecular ions HD^+ and D_2^+ at different energies. The total cross section σ for the production of fragment f is obtained by integra-

tion of $d\sigma_f/d\omega$ over all solid angles as

$$\sigma = 2\pi \int_0^\pi \frac{d\sigma}{d\omega} \sin\theta d\theta. \quad (2)$$

Several runs were made at different gas target pressures and " $d\sigma_f/d\omega$ " was determined for each run. These were compared in order to estimate the reproducibility of the experimental results as well to determine the limits of the "single-collision regime" since the "differential" and total cross sections reported are absolute.

The determinations [5] of the energy distribution of the fragments in the center-of-mass frame of reference and of their angular spread in the laboratory frame (LF) are correlated. This allows an estimation of the binding energy of the molecular projectile, and also the association of some of the prominent structures to the related transitions conducting the excited molecular ion to the dissociation pathways. In doing this, we used the available potential curves for H_3^+ assuming the D_{3h} symmetry [10]. The data were analyzed using the relations [15,13]

$$(M+m)V = M(V_0 - W - E) + mW \pm 2[MmW(V_0 - W - E)]^{1/2}, \quad (3)$$

$$\theta_{\max} = \left[\frac{mW_{\max}}{M(V_0 - W_{\max} - E)} \right]^{1/2}, \quad (4)$$

$$\frac{m}{MV_0} \frac{d\sigma}{d\omega} = f \left[\frac{M}{m} V_0 \theta^2 \right] = f(W). \quad (5)$$

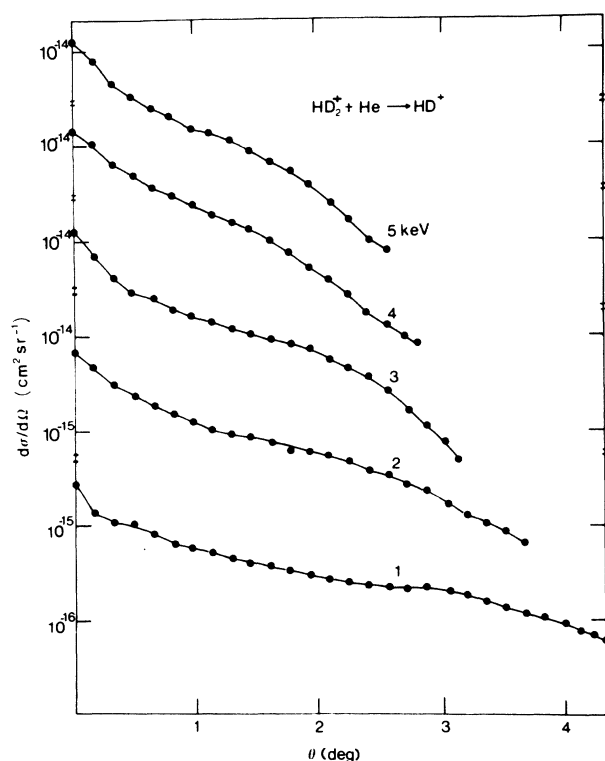


FIG. 1. Angular distributions of the HD^+ fragment as a result of the collision-induced dissociation of the HD_2^+ molecule incident on He.

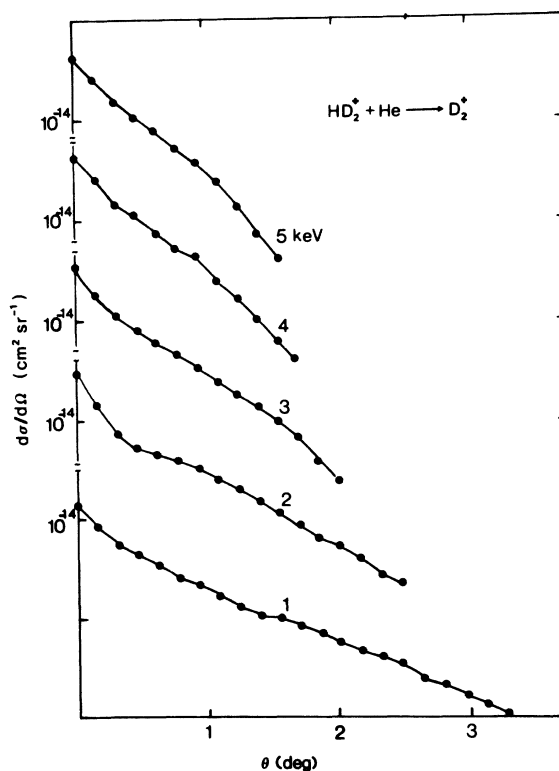


FIG. 2. Angular distributions of the D_2^+ fragment as a result of the collision-induced dissociation of the HD_2^+ molecule incident on He.

Equation (3) refers to energy distributions, whereas Eqs. (4) and (5) refer to angular distributions. In Eq. (3), $(M+m)$ represents the mass of the HD₂⁺ molecular projectile; M , the mass of the detected fragment (HD⁺ or D₂⁺); m , the mass of the undetected fragment (H^{0,+} or D^{0,+}); V is the measured energy of the fragment of mass M detected at an angle of 0° in the LF; V_0 , the initial energy of the molecular projectile; E , the internal energy increase of the system, and W , the kinetic energy released as a result of the dissociation process. The \pm signs correspond to the forward or backward ejection of the fragment of mass M [13,15]. Energy spectra for the HD⁺ and D₂⁺ fragments are shown in Figs. 3 and 4, respectively; the energy of the primary beam was 3 keV.

Equation (4) represents the relation between the maximum kinetic energy W_{\max} of the fragments and their maximum angular spread θ_{\max} . This is the maximum angle between the direction of the primary beam and the direction of the observed fragment (M). Figures 1 and 2 show the position of θ_{\max} , a careful subtraction of the background permits its value to be read directly from the display.

Equation (5) represents a scaling law that relates the angular distributions for different V_0 (incident energies); $d\sigma/d\omega$ (absolute "differential cross section"), and θ (angle between the observed fragment and the incident-beam direction). It has been shown [16,17] that for any fragment arising from a velocity-independent process such as

electronic excitation, the left-hand side of Eq. (5) is a universal function of $(M/m)V_0\theta^2$, which in the present energy range, $V_0 \gg E+W$, becomes a function of W . This result arises from five assumptions, namely that (i) the electronic excitation is faster than both vibrational and rotational times, (ii) rotational energies are negligible in comparison with dissociation energies, so that the dissociation direction is that of the line joining the two fragments, (iii) all orientations are equally probable, (iv) dissociation energies are small in comparison with the incident beam energy, and (v) the deflection of the center of mass of the molecular ion following electronic excitations is negligible. Notice that the above assumptions are the same as those supporting the validity of the two-step model in the keV region [15].

From Eqs. (3) and (4) we can relate the results from both angular and energy-distribution measurements. The angular distribution of the dissociation products is due entirely to the transverse component of the dissociation velocity of the fragment. Thus, with the observed θ_{\max} in the angular distributions, and provided that $V_0 \gg W_{\max} + E$, then W_{\max} is evaluated from Eq. (4), and this value must be the same as that derived from Eq. (3) by taking the energy values at which the intensity reaches a minimum in the energy spectra. It has been pointed out [18] that the maximum in $E+W$ ensures that the excitation originates in the lowest vibrational level of the triatomic ion and the maximum in W ensures the minimum residual internal energy.

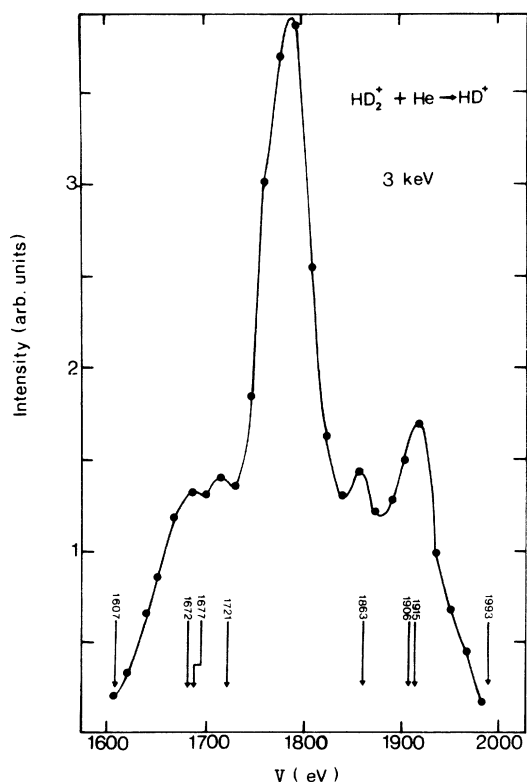


FIG. 3. LF energy spectrum of the HD⁺ fragment at 3 keV and 0° from HD₂⁺ incident on He.

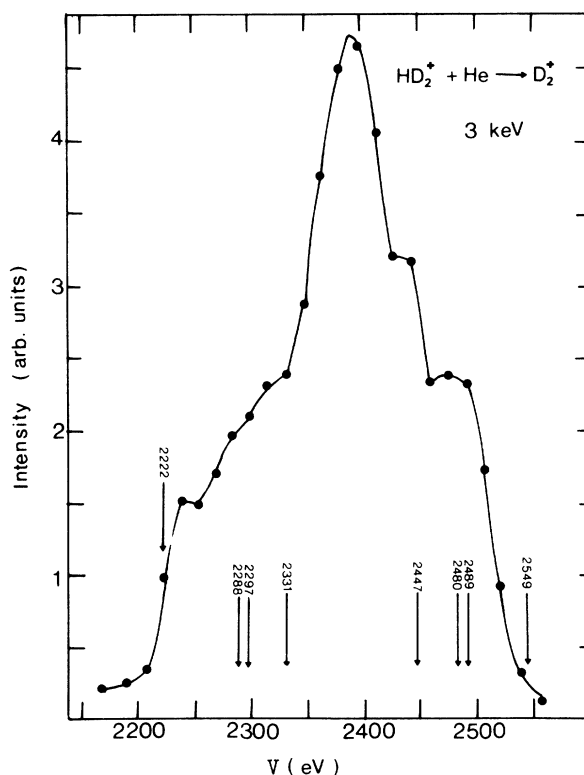


FIG. 4. LF energy spectrum of the D₂⁺ fragment at 3 keV and 0° from HD₂⁺ incident on He.

The spectra of dissociation energies in collision-induced dissociation rarely consist of sharp lines, and the excitation cross sections depend strongly on the instantaneous separation R_{mM} of the molecular constituents M and m at the time of collision. Very often, the spectrum of dissociation energies consists of broad structures or shoulders due to the distribution of vibrational energies in which the projectile enters the collision. A similar explanation holds for angular distributions. The data were treated through an iteration method by taking the energies corresponding to the minimum-intensity limits on the energy spectra as testing values, comparing the corresponding W and E for the two branches of the spectra, and then comparing this W value with the W_{\max} as derived from the angular distributions. Finally the best E and W values compatible with both angular and energy distributions were obtained, with proper regard to the angular and energy resolutions of the experimental apparatus. The analyses of the structure present in the energy spectra were performed only using Eq. (3) because the lack of structure in the angular distributions does not allow any correlation between them. Moreover, the experimental method used is not accurate enough to resolve the multiple contributions of the different states to the spectra, and hence it does not allow a definite assignment to the transitions.

IV. RESULTS AND DISCUSSION

A. The HD^+ fragment

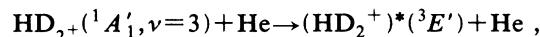
The trial values for the laboratory energies at minimum intensity were taken from Fig. 3, which gave $V_1=1607$ eV and $V_2=1993$ eV. From the angular distributions θ_{\max} was determined (see Fig. 1) and W_{\max} was calculated by Eq. (2). The iteration method already described gave $W=13.5\pm 1.08$ eV and $E=6.4\pm 0.51$ eV.

Two pairs of broad structures on both sides of the central peak are apparent in the energy distribution. For the first pair the LF energy values at the points of maximum intensity were chosen as $V_1=1677$ eV and $V_2=1915$ eV for the backward and forward components of the added velocity, respectively. Applying the method already described, $W=4.92\pm 0.39$ eV and $E=5.43\pm 0.44$ eV were obtained. For the second pair $V_1=1721$ eV and $V_2=1863$ eV were chosen, which results in $W=1.76\pm 0.14$ eV and $E=12.59\pm 1.01$ eV.

Figure 5 exhibits the transitions suggested through the E and W values derived from the distributions. Using the same theoretical potential curves as for H_3^+ [19], the governing transition at the points of minimum intensity in both angular and energy distributions goes from the $^1A_1'$ ground state of HD_2^+ to the $^1E'$ repulsive state. Our determined value for the internal energy E agrees well with theoretical calculations and experimental measurements for the binding energy of the H_3^+ molecular ion [13].

The first outer pair of broad structures can be interpreted as follows: the $^3E'$ state is repulsive, and since it is known that when a triangular molecule as H_3^+ undergoes a small distortion from the D_{3h} to the C_{2v} symmetry

due to a collision, it splits into the 3A_1 and 3B_2 states, thereby producing H_2^+ (HD^+ or D_2^+ for the HD_2^+ case) as a charged fragment. In this case



proceeding to

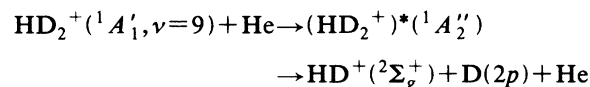


or



By slightly varying the V values to $V_1=1672$ eV and $V_2=1906$ eV, $W=4.8\pm 0.38$ eV and $E=16.76\pm 1.34$ eV was obtained. A possible transition on the potential surfaces is that leading to the excited $(\text{HD}_2^+)^*(^1A_2'')$ state followed by the dissociation into the $\text{HD}^+(^2\Sigma_g^+) + \text{D}(2p)$ products.

For the second pair, the reaction



fits well on the potential curves. All of these possible transitions are shown in Fig. 5.

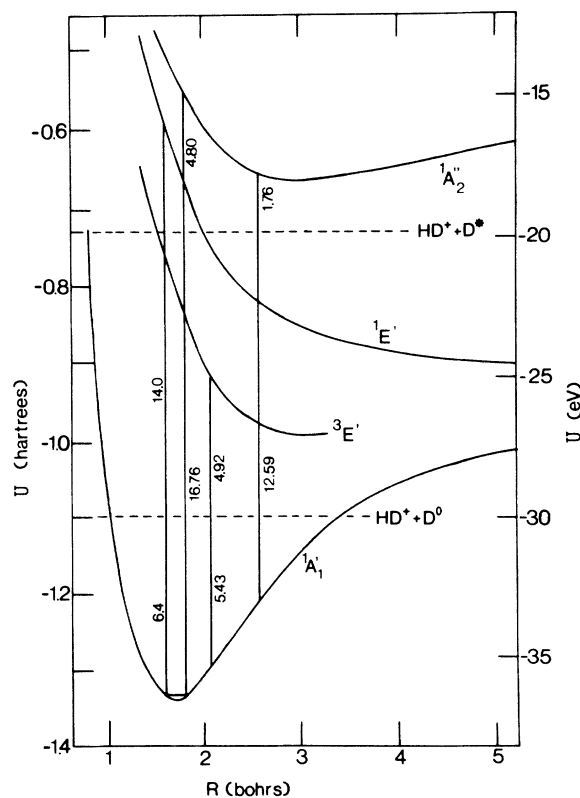
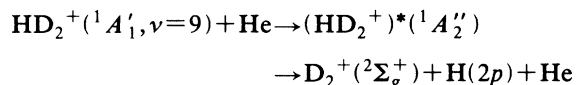


FIG. 5. Relevant HD_2^+ potential-energy curves (assuming D_{3h} -symmetry equilateral triangle, as for H_3^+ in Ref. [19]). R is the length of the side of the triangle. Dotted lines show the dissociation limits.

B. The D₂⁺ fragment

The LF energy spectra of the D₂⁺ fragments are shown in Fig. 4. The position of the minimum-intensity points has been selected as follows: $V_1=2222$ eV and $V_2=2549$ eV. With these values, and θ_{\max} from the angular distributions (Fig. 2), following the method already described values of $W=14\pm 1.2$ eV and $E=6.5\pm 0.52$ eV for the kinetic energy released and for the internal energy were obtained.

Even though the D₂⁺ spectrum is different than that of HD⁺, two poorly defined pairs of structures can still be seen. One of them at $V_1\approx 2331$ eV and $V_2\approx 2447$ eV and the other estimated at $V_1\approx 2288$ eV and $V_2\approx 2480$ eV. With these values we obtain $W=1.76\pm 0.14$ eV and $E=12.67\pm 1.01$ eV for the outer structure and $W=4.81\pm 0.39$ eV with $E=16.85\pm 1.35$ eV for the inner structure. The proposed transitions consistent with these values are



for the inner structure, and

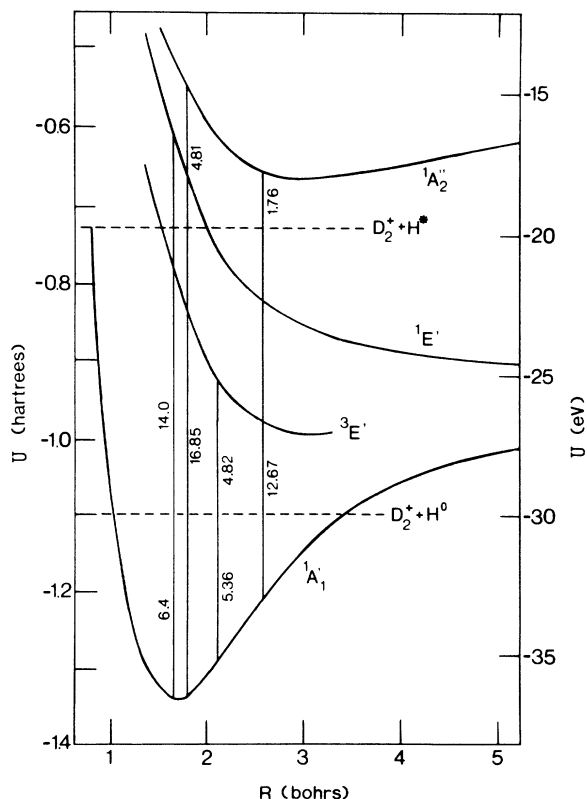
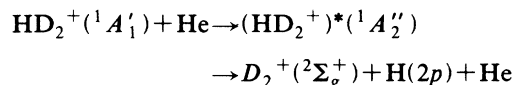
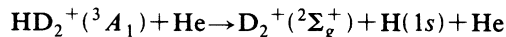
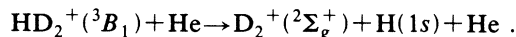


FIG. 6. Relevant HD₂⁺ potential-energy curves (assuming D_{3h}-symmetry equilateral triangle, as for H₃⁺ in Ref. [19]). R is the length of the side of the triangle. Dotted lines show the dissociation limits.

for the outer structure. Other possible transition compatible with the measured V values can be obtained by allowing small changes close to the chosen V values. For example, for the outer shoulder, with $V_1=2297$ eV and $V_2=2489$ eV, then $W=4.82\pm 0.39$ eV and $E=5.36\pm 0.43$ eV are obtained, matching the transition $\text{HD}_2^+(^1A'_1, \nu=3) + \text{He} \rightarrow (\text{HD}_2^+)^*(^3E') + \text{He}$, leading to the channel



or



The results for D₂⁺ are displayed in Fig. 6.

C. The angular distributions and total cross sections of the HD⁺ and D₂⁺ fragments

Plotted in Figs. 7 and 8 are the angular distributions of the HD⁺ and D₂⁺ fragments as a function of the reduced variables in Eq. (5). It is noted that within the experimental error, all the angular distributions scale according to this equation. Thus, it is reasonable to infer that over the energy range explored, the same processes are taking place. However, in both figures a systematic departure is observed for the diatomic fragments at 1 keV. This behavior may be due to a deviation from the bases supporting the two-step process, one may cite, for example, a deviation of the center-of-mass motion of the fragments

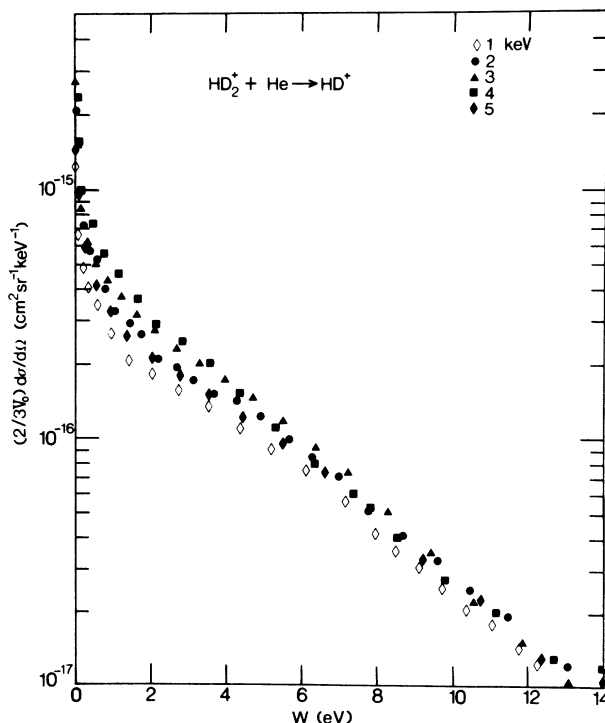


FIG. 7. Single-run scaled angular distributions of the HD⁺ fragment. Horizontal axis shows the $W (=MV_0\theta^2/m)$ energy values.

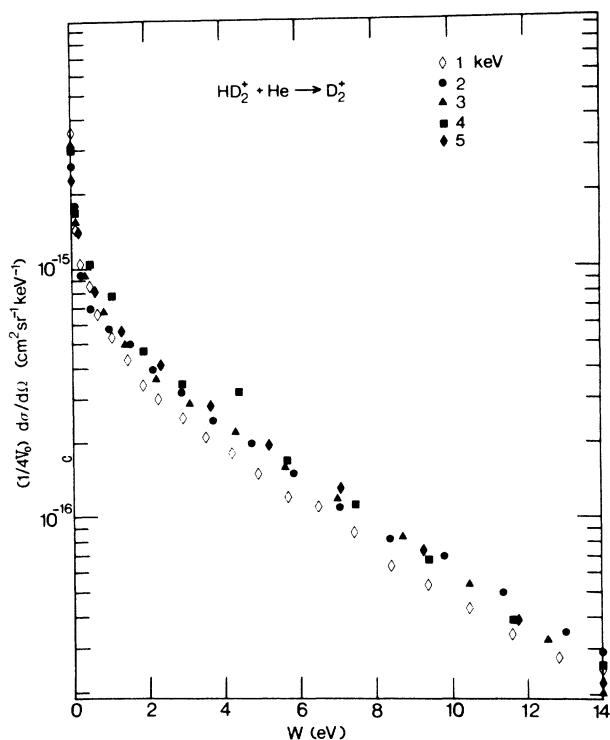


FIG. 8. Single-run scaled angular distributions of the D_2^+ fragment. Horizontal axis shows the $W (=MV_0\theta^2/m)$ energy values.

produced in the collision at low energies.

Figure 9 displays the total cross sections obtained from integration of the differential cross sections [Eq. (2)]. The trends for both fragments are the same but the cross sections for the production of D_2^+ are roughly a factor of 1.5 on average higher than that of HD^+ . This fact is indicative of a weaker bond of HD^+ with respect to that of the D_2^+ fragment.

The results of the present work can be summarized as follows.

(a) We have presented the differential cross sections and the absolute total cross sections for the production of the D_2^+ and HD^+ fragments from the reaction $HD_2^+ + He$.

(b) From the angular and energy distributions of the dissociation products HD^+ and D_2^+ we were able to measure the binding energy of the HD_2^+ molecule. The average of the determined $(W + E) = 20.15 \pm 1.64$ eV is basically the energy needed to raise the H_3^+ to an intermediate unbound state, in agreement with theory for the $^1E'$ state for the equilateral-triangle configuration. Additionally, from the structure in the energy distributions

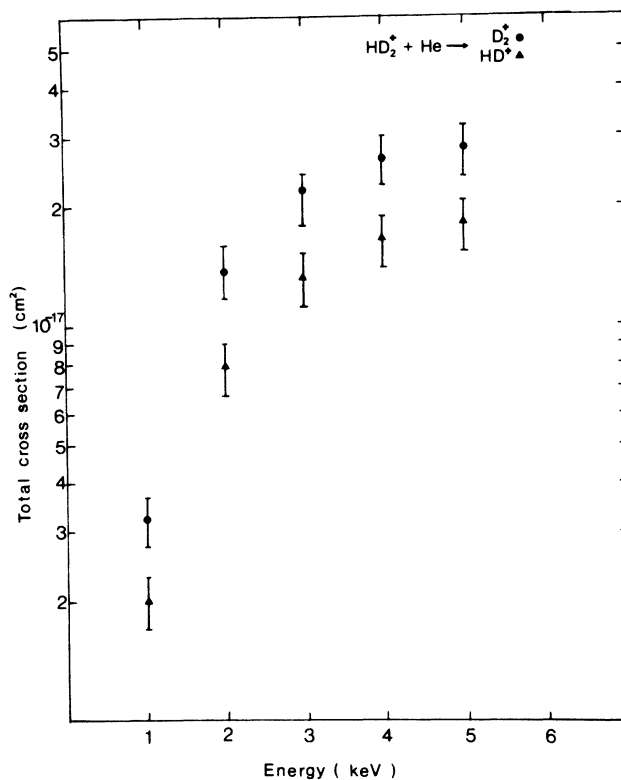


FIG. 9. Absolute total cross sections for the production of the HD^+ and D_2^+ fragments produced by the collision-induced dissociation of HD_2^+ in He.

some possible dissociation channels could be identified and were found to be the same for both fragments. The different shapes of the distributions result from different intensities due to the mass effect.

(c) The departure of the differential cross sections at 1 keV from the scaling law may be an indication that at this low energy of the incoming beam some of the assumptions supporting the two-step-process model are no longer valid.

(d) The mass effect is also apparent in the total cross sections, together with the fact that the difference in the probability for production of the two fragments is the result of the different binding-energy values of D_2^+ and the HD^+ components in the molecule.

ACKNOWLEDGMENTS

The authors wish to thank S. Pérez for his technical assistance. This work has been partially supported by DGAPA Grant No. IN-01-48-89 and by Consejo Nacional de Ciencia y Tecnología.

[1] E. Herbst and W. Klemperer, *Astrophys. J.* **185**, 505 (1973).

[2] W. D. Watson, *Rev. Mod. Phys.* **48**, 513 (1976).

[3] E. Herbst and W. Klemperer, *Phys. Today* **20**, 32 (1976).

[4] D. Smith, N. G. Adams, and E. Alge, *Astrophys. J.* **263**,

123 (1982).

[5] J. B. Mitchell, T. C. Ng, L. Forand, R. Janssen, and J. Wm. McGowan, *J. Phys. B* **17**, L909 (1984).

[6] I. Alvarez, C. Cisneros, J. A. Ray, C. F. Barnett, and A. Russek, in *Proceedings of the XI International Conference*

- on the Physics of Electronic and Atomic Collisions, Kyoto, 1979*, edited by K. Takayanagi and N. Oda (The Society for Atomic Collision Research, Kyoto, 1979), p. 910.
- [7] I. Alvarez, C. Cisneros, C. F. Barnett, and J. A. Ray, *Phys. Rev. A* **14**, 602 (1976).
- [8] G. Astner, S. Mannervick, and E. Veje, *Phys. Rev. A* **25**, 828 (1982).
- [9] A. Carrington and R. A. Kennedy, *J. Chem. Phys.* **81**, 91 (1984).
- [10] B. A. Colling, J. E. Polany, M. A. Smith, A. Stolow, and A. W. Tarr, *Phys. Rev. Lett.* **59**, 2551 (1987).
- [11] G. D. Carney and R. N. Porter, *Chem. Phys. Lett.* **50**, 327 (1977).
- [12] M. Berlinger, J. M. Gomez-Llorente, E. Pollak, and Ch. Schlier, *Chem. Phys. Lett.* **146**, 353 (1988).
- [13] H. Martínez, I. Alvarez, J. de Urquijo, C. Cisneros, and A. Amaya-Tapia, *Phys. Rev. A* **36**, 5425 (1987).
- [14] G. A. Harrower, *Rev. Sci. Instrum.* **26**, 850 (1955).
- [15] J. Los and T. R. Govers, in *Collision Spectroscopy*, edited by R. G. Cook (Plenum, New York, 1978), p. 289.
- [16] C. Cisneros, I. Alvarez, C. F. Barnett, J. A. Ray, and A. Russek, *Phys. Rev. A* **14**, 88 (1976).
- [17] C. Cisneros, I. Alvarez, R. García, C. F. Barnett, J. A. Ray, and A. Russek, *Phys. Rev. A* **19**, 631 (1979).
- [18] S. C. Goh and J. B. Swan, *Phys. Rev. A* **24**, 1624 (1981).
- [19] K. Kawaoka and R. F. Borkman, *J. Chem. Phys.* **54**, 4234 (1971).